This is the author's peer reviewed, accepted manuscript. However, the online version of record will be different from this version once it has been copyedited and typeset

# Dean Vortex-Enhanced Blood Plasma Separation in Self-Driven Spiral Microchannel Flow with Cross-Flow Microfilters

Yudong Wang a, Niladri Talukder a, Bharath Babu Nunna b,c,d, and Eon Soo Lee \*a

- <sup>a</sup> Advanced Energy Systems and Microdevices Laboratory, Department of Mechanical and Industrial Engineering, New Jersey Institute of Technology, Newark, NJ 07102, USA.
- <sup>b</sup> Department of Mechanical Engineering, Weber State University, Ogden, UT-84408, USA.
- <sup>c</sup> Division of Engineering in Medicine, Department of Medicine, Brigham and Women's Hospital, Harvard Medical School, Harvard University, Cambridge, MA 02139, USA
- <sup>d</sup> Harvard Graduate School of Education, Harvard University, Cambridge, MA, USA-02138
- \*Corresponding author: Department of Mechanical and Industrial Engineering, New Jersey Institute of Technology, NJ, 07102, USA; Tel: +1 973 596 3318; E-mail: eonsoo.lee@njit.edu

## **♦** Abstract

Point-of-care (POC) diagnostic devices have been developing rapidly in recent years, but they are mainly using saliva instead of blood as a test sample. A highly efficient self-separation during the self-driven flow without power systems is desired for expanding the Point-of-care diagnostic devices. Microfiltration stands out as a promising technique for blood plasma separation but faces limitations due to blood cell clogging, resulting in reduced separation speed and efficiency. These limitations are mainly caused by the high viscosity and hematocrit in the blood flow. A small increment in the hematocrit of the blood significantly increases the pressure needed for the blood plasma separation in the micro-filters and decreases the separation speed and efficiency. Addressing this challenge, this study explores the feasibility of diluting whole blood within a microfluidic device without external power systems. This study implemented a spiral microchannel utilizing the inertial focusing and Dean vortex effects to focus the red blood cells and extract the blood with lower hematocrit. The inertial migration of the particles during the capillary flow was first investigated experimentally; a maximum of 88% of the particles migrated to the bottom and top equilibrium positions in the optimized 350 x 60 µm (cross-sectional area, 5.8 aspect ratio) microchannel. With the optimized dimension of the microchannel, the whole blood samples within the physiological hematocrit range were tested in the experiments, and more than 10% of the hematocrit reduction compared between the outer branch outlet and inner branch outlet in the 350 x 60 µm microchannel.

PLEASE CITE THIS ARTICLE AS DOI: 10.1063/5.0189413

### Introduction

Point-of-care (POC) diagnostic devices are ideally rapid, easy-to-use, low cost, and accurate for disease antigen or nucleic acid detection. Over the past decade, there has been a growing interest in POC disease diagnostic devices, with POC technology being applied for the rapid detection of many diseases [1]. However, the expansion of POC technology applications is restrained by certain technical barriers, particularly in cases where biomarkers need to be detected in blood plasma to ensure high detection accuracy [2-6]. A self-powered standalone blood plasma separation technique adapted to the POC applications is highly desired to address these technical barriers and expand the at-home test device to the broader detection of diseases [7]. Most blood plasma separation microfluidic devices rely on external devices and functionalities such as syringe pumps, magnetic forces, dielectrophoretic forces, acoustic forces, etc [8-11]. In contrast to most microfluidic devices, the blood plasma self-separation platform operates independently, without relying on external pumping systems or additional functionalities [12]. The pre-vacuumed microchannel space attached to the main microchannel and the capillary action induced by the modified microchannel surface are the primary techniques for propelling blood flow in the microchannel. To implement pre-vacuumed microchannels for self-pumping the blood flow in the microchannel, Dimov et al. utilized a pre-vacuumed PDMS microchannel to establish a pressure gradient between atmospheric pressure and the pressure within the microchannel, driving the blood flow within the microchannel [13]. By implementing the filter trench, the blood cells were sendimented, and the plasma was extracted forward in the microchannel. Yeh et al. employed a vacuum battery, involving a vacuumed microchannel attached to the main microchannel, to propel the blood sample within the microchannel and facilitate the separation of plasma by sedimenting the blood cells in the microwell and extracting plasma through microfilters [14]. In their technologies, the separation time is relatively longer due to the low flow rate and the requirement for blood cell sedimentation. Beside pre-vacuumed microchannel, the capillary action also can serve as the driving force for fluid flow within the microchannel [15]. By modifying the hydrophilicity of the channel surface, the biofluid is able to flow into the microchannel spontaneously [16]. Maria et al. introduced

PLEASE CITE THIS ARTICLE AS DOI: 10.1063/5.0189413

a hydrophobic patch in the surface-modified hydrophilic microchannel [17]. The blood flow was driven by the capillary pressure induced by the hydrophilic microchannel. In the hydrophobic patch, plasma separated out due to the higher flow speed resulting from the lower viscosity compared to the blood cells, while the blood cells were trapped in the hydrophobic patch. However, this technique is limited by the characteristics of blood samples and is challenging to directly apply to Point-of-Care (POC) applications. Researchers have explored microchannel dimensions and geometries to leverage hydrodynamic forces for blood plasma separation, employing techniques such as inertial migration and Dean vortex [18-20]. However, these methods still rely on the consistent flow rate of the blood provided by external pumping systems, as the fluid's flow rate directly influences the lift and drag forces exerted on the blood cells.

Unlike the flow driven by external pumping systems, capillary flow exhibits inconsistent flow rates due to pressure drops resulting from increasing viscous forces within the microchannel [21-23]. Consequently, the use of inertial focusing or other hydrodynamic forces for blood plasma separation is constrained in capillary flow due to its inconsistent and insufficient flow rate [24]. The microfilters recently became one of the most popular technologies for blood plasma separation in microchannels with self-driven flow [25]. Various microfiltration designs have been developed to achieve blood plasma separation within microfluidic systems [26-32]. However, these microfilters have their limitations. Dead-end and membrane filters are susceptible to clogging by blood cells, leading to reduced separation speed and yield [33]. While cross-flow filters can mitigate the clogging issue, separation speed remains limited, particularly when filtering blood samples with a high hematocrit (volumetric percentage of red blood cells in whole blood) [34].

In the context of blood plasma separation using microfilters, lower hematocrit levels are always preferred to achieve higher separation speeds, primarily due to the decreased viscosity of blood influenced by the quantity of red blood cells (RBCs) [35,36]. In microchannels with tiny microfilter dimensions (~2 µm), even slight increases in hematocrit within the blood sample lead to a noticeable pressure difference within the

filters, caused by changes in blood flow viscosity [37-40]. The complexities of blood viscosity, influenced by RBC shape changes and the formation of RBC rouleaux due to cell aggregations, especially under low shear rate conditions (<100 s<sup>-1</sup>), highlight the critical role of hematocrit [35, 41]. At higher shear rates, RBCs change shape, becoming flatter and aligned with the flow, reducing resistance to blood flow and breaking apart RBC rouleaux. Nonetheless, hematocrit remains a significant factor influencing blood viscosity [42]. The work of Weiss et al. reported the considerable impact of hematocrit, showing a threefold increase in pressure requirements for blood with a 60% hematocrit compared to that with a 36% hematocrit [37]. Even a small 1% increase in hematocrit raises blood viscosity by 4% under high shear rate conditions [42]. As most self-driven-flow-based microfiltration devices operate within a low shear rate range [43], the influence of hematocrit on blood viscosity becomes more pronounced. The significant effect of hematocrit on blood viscosity, combined with the potential for additional RBC cluster formation in the flow, highlights the need to minimize the blood hematocrit to prevent delays in blood plasma separation and filter clogging [44]. Hence, achieving a slight (5-10%) reduction is well expected to lead to a substantial increase in blood plasma separation in the microfilter settings, and this approach for the microfilter settings emerges as a promising strategy.

In the field of inertial microfluidics, the effects of inertial focusing and Dean vortex on particle migration have been explored, particularly in channels orchestrated by pumping systems [45-50]. However, a gap exists in understanding these phenomenon within the confinement of capillary flow conditions in microchannels. Unlike the controlled environments with the assistance of pumping systems where meticulous manipulation of flow rate can be achieved, the efficacy of the inertial microfluidic phenomenon in capillary flow conditions remains unclear [51, 52]. While the pricise control of the particles is more difficult to achieve in the capillary flow due to the dynamic change of the advancing velocity of the meniscus than in the constant flow rate condition where the flow velocity field is maintained constant, the potential of inertial focusing of RBCs emerges as a promising method for controlling hematocrit in a self-driven flow environment [53].

This is the author's peer reviewed, accepted manuscript. However, the online version of record will be different from this version once it has been copyedited and typeset

This study focuses on the blood hematocrit reduction under capillary flow conditions implementing inertial focusing and the Dean vortex phenomenon in an optimized spiral microchannel. The primary novelty lies in the exploration of inertial focusing and Dean vortex applications for the blood plasma self-separation in microchannels and micro-structured settings, coupled with a rigorous quantitative analysis of blood plasma separation. The experiments using whole blood within the physiological range were conducted in the microchannel optimized by iterative adjustments to the microchannel geometry to quantify the separation of RBCs. Initial study was performed with blood mimicking fluid (BMF) to understand the particle dynamics, and implemeted on the whole blood condition. This paper presents the experimental study on the inertial focusing and Dean vortex of the blood cell in the spiral microchannel capillary flow for enhancement of blood plasma separation in microfilters, and provides a reference for the self-separation microfluidic system design without external devices involved.

### **◆** Materials and methods

#### **Materials**

Indium Tin Oxide (ITO) coated glass slides and IP-S photoresist resin were procured from Nanoscribe, while 9.5 µm polystyrene microspheres were obtained from Cospheric LLC. Porcine whole blood was sourced from Lampire Biological Laboratories. Sylgard 184 Silicone Elastomer and its curing agent were purchased from Dow Corning.

#### **Microfluidic Devices Working Principle**

In inertial microfluidics, it is a prerequisite for the Reynolds number (Re) to exceed 1 to ensure that both inertial and viscous forces are effective in the flow. This criterion, however, imposes limitations on the length of microchannels when dealing with capillary flow due to the declining flow rate within the channel. Based on experimental results, microchannels with a depth of 60  $\mu$ m and varying widths of 250  $\mu$ m, 350  $\mu$ m, 450  $\mu$ m, and 550  $\mu$ m have constrained lengths ranging from 22 mm to 32 mm. Due to this limitation, the length of all microchannels was uniformly designed to be 22 mm. The hydraulic diameter of the microchannel is also constrained by the target particle size. To

This is the author's peer reviewed, accepted manuscript. However, the online version of record will be different from this version once it has been copyedited and typeset

ensure effective particle migration, the ratio of particle size to hydraulic diameter should exceed 0.07 [51]. Given that red blood cells (RBCs) are targets for separation, with an average diameter of 8  $\mu$ m at their largest portion, the maximum hydraulic diameter of the microchannel is restricted to 114  $\mu$ m. Another limiting factor is the radius of curvature of the microchannel, which is influenced by the available space between each turn of the spiral. As a maximum 550  $\mu$ m-width microchannel was designed in the experiment setup, the radius difference between two spiral turns should be more than 600  $\mu$ m to ensure the spacing between the neighbor spiral microchannel is bigger than 50  $\mu$ m for practical microchannel fabrication. Based on these considerations, a spiral configuration was designed by the equation (1):

$$r = 0.6 + \theta/540$$
 (1)

Where r is the radius in mm of spiral from in to out,  $\theta$  is defined from  $0^{\circ}$  to  $1080^{\circ}$  which means 3 turns of the spiral. The spiral channels were meticulously designed and fabricated for the purpose of investigating particle focusing during capillary flow. These microchannels possessed cross-sectional dimensions of 250 x 60  $\mu$ m, 350 x 60  $\mu$ m, 450 x 60  $\mu$ m, and 550 x 60  $\mu$ m, with a uniform length of 22 mm. The average radii along the path from the inlet to the outlet are 0.6 mm, 1.3 mm, and 2.0 mm for the respective three turns, as depicted in the figure 1.

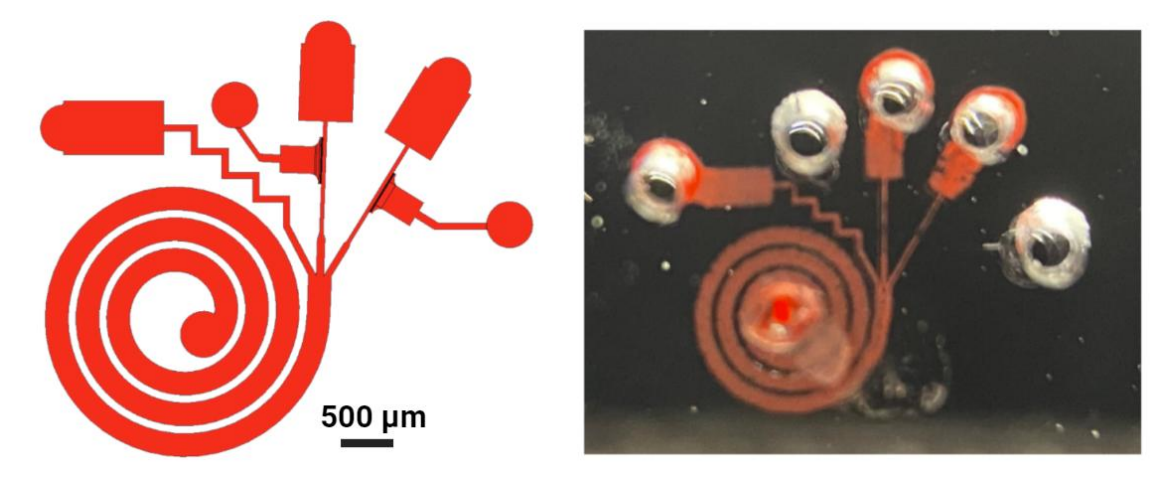


Figure 1. Spiral Microchannel design (left) and the Spiral Microchannel after the experiment (right).

#### **Microfluidic Devices Fabrication**

PLEASE CITE THIS ARTICLE AS DOI: 10.1063/5.0189413

The master molds of the microchannels were fabricated with the Photonic Professional GT, made by Nanoscribe. The Photonic Professional is a two-photon polymerization system designed to produce micro or sub-micro structures. The specific process used in this work was Dip in Laser Lithography (DiLL), where the optics focusing the laser used to cross-link the resist are inserted directly into the resist. This minimizes optical distortion of the laser and helps ensure peak accuracy of the final features.

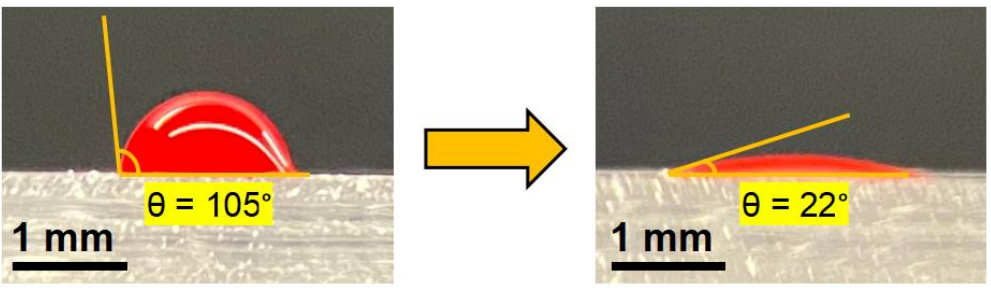
The microchannels were then fabricated using soft-lithography method with Polydimethylsiloxane (PDMS). The Sylgard 184 Silicone Elastomer and its curing agent are mixed thoroughly at the mass ratio of 10:1 and ensure the curing agent is homogeneously distributed in the mixture to make the PDMS uniformly cross-linked. After the PDMS mixture is prepared, pour the PDMS mixture on the microchannel master mold in a glass container and place the container into a vacuum chamber to degas the PDMS mixture. Once complete the degassing, the container is replaced from the vacuum chamber to the oven and baked at 70°C for 3 hours to accelerate the cross-linking reaction in the PDMS mixture and cure the PDMS slab. When the PDMS is appropriately cured, carefully detach the PDMS slab from the master mold and use the puncher to punch the inlet and outlet ports of the microchannel. The PDMS slab with a microchannel was fabricated to be 1.5 mm in thickness, and all the inlet and outlet ports are 1 mm in diameter. In all experiments, the 2 µl of BMF and blood samples are dropped into the microchannel through the inlet without additional pressure and driven by capillary pressure along the hydrophilic microchannel wall towards the outlets.

#### **Surface Treatment of Microchannels**

The surface of the PDMS microchannel is naturally hydrophobic. However, a hydrophilic surface is necessary to activate the capillary action and make the fluid naturally flow inside the microchannel. When the PDMS slab is exposed to the oxygen plasma, oxidation occurs on the surface. This process involves the removal of organic and hydrocarbon materials from the PDMS surface through chemical reactions with reactive oxygen radicals and the physical removal by energetic oxygen ions. As a result of oxidation, the surface of PDMS develops silanol (SiOH) groups, which make the surface

PLEASE CITE THIS ARTICLE AS DOI: 10.1063/5.0189413

more hydrophilic. The PDMS surface Oxygen plasma treatment was conducted in a vacuum chamber below 1 Torr of surrounding air. A criteria of 60-second treatment is used to ensure the consistency of every experimental condition. The blood contact angle on the PDMS surface changed from 105° to 22°, as show in figure 2.



# **Oxygen Plasma Treatment**

Figure 2. Contact angle measurements of the blood drops on the PDMS surface before (left) and after (right) Oxygen plasma treatment. The PDMS surface was converted from hydrophobic nature to hydrophilic.

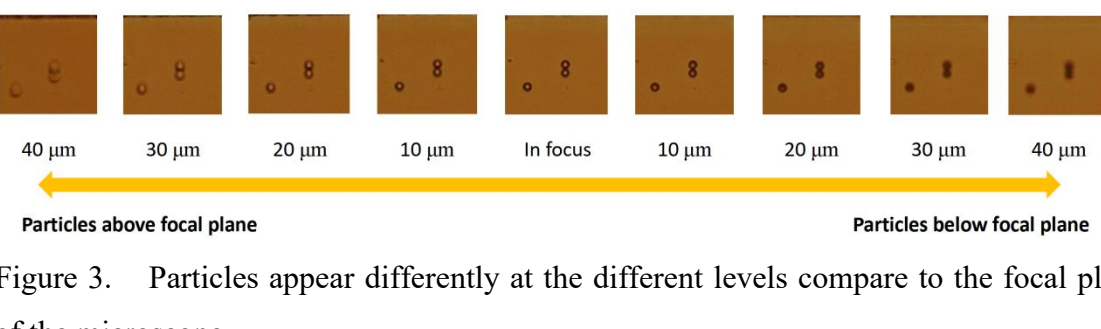
#### **Blood sample preparation**

The Porcine blood samples were purchased from Lampire Biological Laboratories. The blood samples were first centrifuged at 3500 rpm for 30 minutes to separate plasma and blood cells. Subsequently, the hematocrit level of the original samples was recorded. The desired blood samples with hematocrit levels of 30%, 35%, 40%, and 45% were then prepared by either adding or removing plasma from the original blood samples to achieve the specified hematocrit values for the experiments.

#### Image processing tool for particle counting

In the microscope view, the particles above the focal level, in the focal level, and below the focal level have the different appearances in the frames recorded by the high-speed camera. The particles appearances at the different levels compare to the microscope focal plane are shown in the figure 3.

PLEASE CITE THIS ARTICLE AS DOI: 10.1063/5.0189413



Particles appear differently at the different levels compare to the focal plane of the microscope.

In the imaging analysis, particles located within the focal plane exhibit characteristics akin to clear circular rings. As one moves above the focal plane, these particles gradually transform into increasingly blurred ring-like shapes, while those situated below the focal plane present themselves as solid rounds that gradually fade. Leveraging these distinct features, an imaging processing method has been employed to analyze the video frames of the flowing particles and quantify their state of focus. This method entails a two-step image processing procedure, as illustrated in Figure 4.

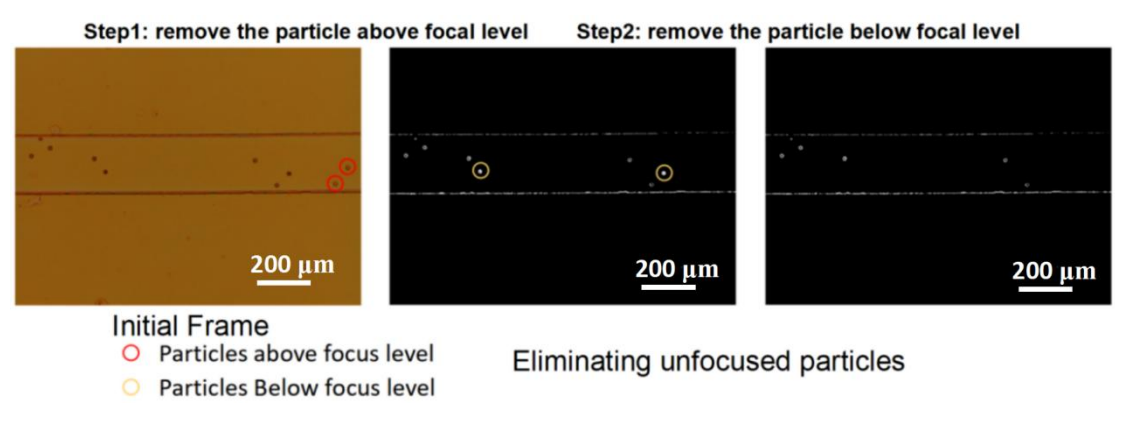


Figure 4. The image processing method to count the in-focus particles and total particles in a frame.

The image processing method employed a two-step approach for particle analysis. In the initial step, particles located above the focal plane (characterized as blurry circles) were removed using a binary technique, while converting the Red, Green, and Blue color (RGB) image to grayscale. In the second step, particles below the focal plane (resembling blurry solid circles) were eliminated through a method that involved dividing the image into 3 x 3-pixel groups. If all pixels within a group were assigned a value of 1

This is the author's peer reviewed, accepted manuscript. However, the online version of record will be different from this version once it has been copyedited and typeset

(normalized grayscale value, indicating white color in the binary image), that group of pixels was collectively assigned a value of 0 (black). This procedure effectively removed particles positioned below the focal level from the image. Consequently, particles within the focal plane could be accurately quantified. Furthermore, the particle in-focus/out-of-focus ratio could be calculated at various levels of channel height. For instance, when the objective lens was focused at the 25% of the channel height, the relative ratio of particles migrating to the bottom equilibrium position could be quantified.

#### **♦** Results and discussions

The capillary flow in the microchannel is characterized with Reynolds number (Re). The microchannels are treated with air plasma to obtain the hydrophilic surfaces for the capillary flow. The capillary flow speed of the BMF (dynamic viscosity = 3 cP), was measured within microchannels featuring varying aspect ratios (Width/Height) of 4.2, 5.8, 7.5, and 9.2, all possessing a channel depth of 60  $\mu$ m. The hydraulic diameters of these microchannels were computed as 96.77  $\mu$ m, 102.44  $\mu$ m, 105.88  $\mu$ m, and 108.19  $\mu$ m. The Reynolds number (Re) along the length of the channel can be calculated using Equation (2).

$$Re = \frac{\rho v D_h}{\mu}$$
 (2)

Where  $\rho$  is the density of the fluid, v is the flow velocity in the microchannel,  $D_h$  is the hydraulic diameter of the microchannel,  $\mu$  is the dynamic viscosity of the fluid. For microchannels of various sizes and aspect ratios (AR), we recorded data for four distinct positions of BMF travel starting from the channel inlet. The resulting Reynolds numbers for BMF flow within these microchannels at multiple travel lengths have been graphically represented in Figure 5.

This is the author's peer reviewed, accepted manuscript. However, the online version of record will be different from this version once it has been copyedited and typeset

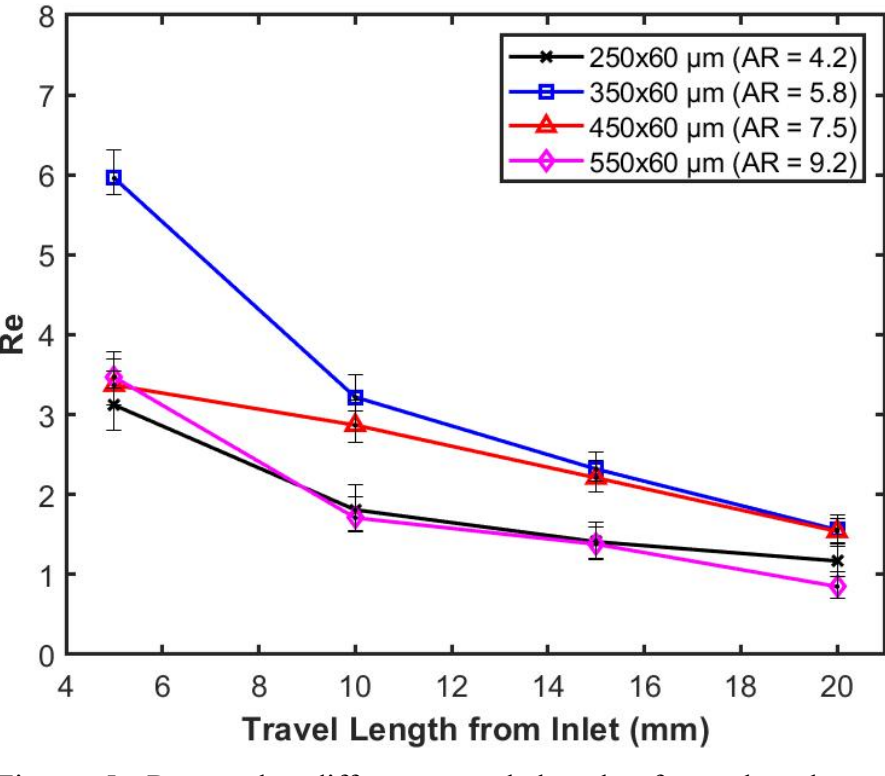


Figure 5. Re at the different travel lengths from the channel inlet in multiple microchannels with various sizes and aspect ratios.

The inertial migration and Dean vortex effect of the particles in the microchannel both rely on the higher Re (but < 100, to ensure both the viscous and inertial effects of the flow in the channel) in the microchannel. Analysis of the data shows that the 5.8 aspect ratio microchannel maintains a higher Reynolds number over its length, promoting favorable conditions for inertial migration and the Dean vortex effects in particle separation within the microchannel. For the experimental setup, a 0.1% particle concentration BMF containing particles with a diameter of 9.5  $\mu$ m was introduced into the microchannels. These flow conditions were recorded by a high-speed camera through an inverted microscope with a magnification of 200x. The focal plane of the microscope was adjusted to the 25% height of the microchannel (15  $\mu$ m from the channel bottom) to monitor and enumerate the particles located near the bottom equilibrium position. Data on the relative particle concentration (the number of particles in the focal plane relative to the total particle count within the frame) at different travel lengths near the bottom

PLEASE CITE THIS ARTICLE AS DOI: 10.1063/5.0189413

equilibrium position in microchannels of various sizes were collected and graphically represented in Figure 6.

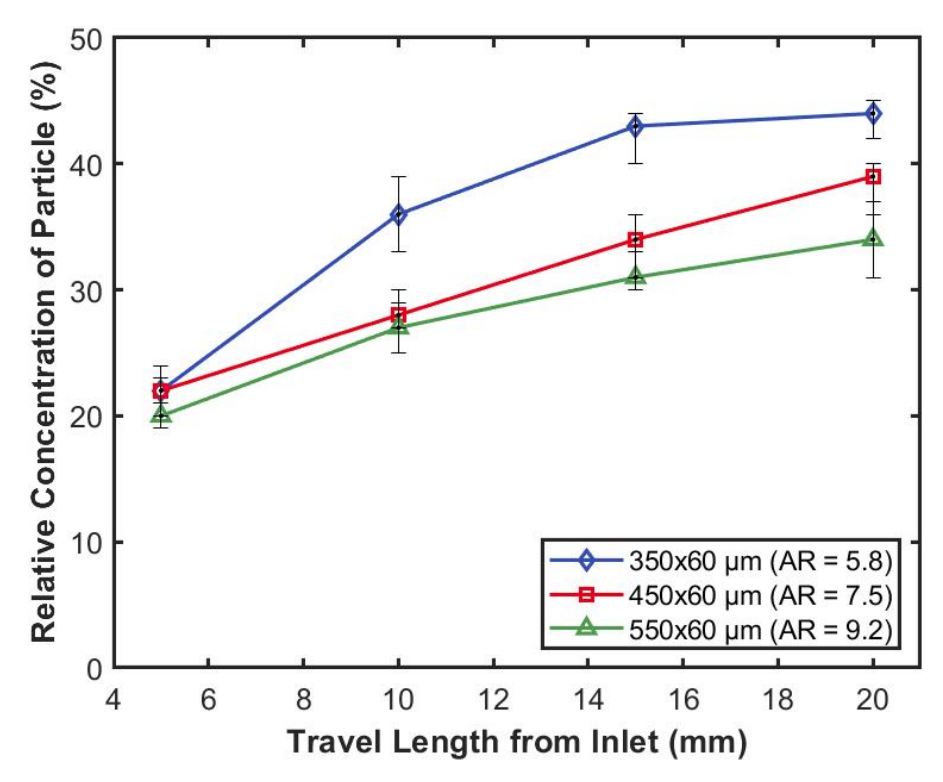


Figure 6. Particle relative concentration near the bottom equilibrium position at multiple travel lengths from the inlets of microchannels with various sizes and aspect ratios.

The 5.8 aspect ratio microchannel exhibited a higher overall flow speed, leading to a relatively greater net lift force acting upon the particles compared to the other microchannels. Additionally, due to the identical channel height across all microchannels, the migration distances of the particles in these channels remained comparable. Consequently, the 5.8 aspect ratio microchannel demonstrated better particle migration efficiency, with approximately 44% of the particles successfully reaching the bottom equilibrium position. Considering the negligible influence of gravity in microfluidic flows, it is reasonable to assume symmetric migration of particles to both the top and bottom sides. In the 5.8 aspect ratio microchannel, a notable 88% of particles reached their respective equilibrium positions, a higher percentage compared to 78% in the 7.5 aspect ratio microchannel and 68% in the 9.2 aspect ratio microchannel.

PLEASE CITE THIS ARTICLE AS DOI: 10.1063/5.0189413

In the spiral microchannel, Dean number (De) plays a critical role to describe the intensity of the Dean vortices which can be expressed by equation (3).

$$De = Re \sqrt{\frac{D_h}{2R_c}}$$
 (3)

Where Re is the Reynolds number, Dh is the hydraulic diameter, and Rc is the radius of curvature of the spiral channel. As shown in the equation (3), De is proportional to the Re and the hydraulic diameter Dh, and counter proportional to the radius of curvature of the spiral channel [54]. Since the Re is limited by the capillary flow nature, and Dh is limited by the size of the targeted particle for the separation, the Rc is designed as small as possible to enhance the Dean vortices effect on the particles in the microchannels with various sizes. To gain a comprehensive understanding of the relationship between the Dean number and travel length, we plotted Dean numbers against travel lengths for microchannels featuring diverse sizes and aspect ratios. The representation of the De versus travel length is plotted in Figure 7.

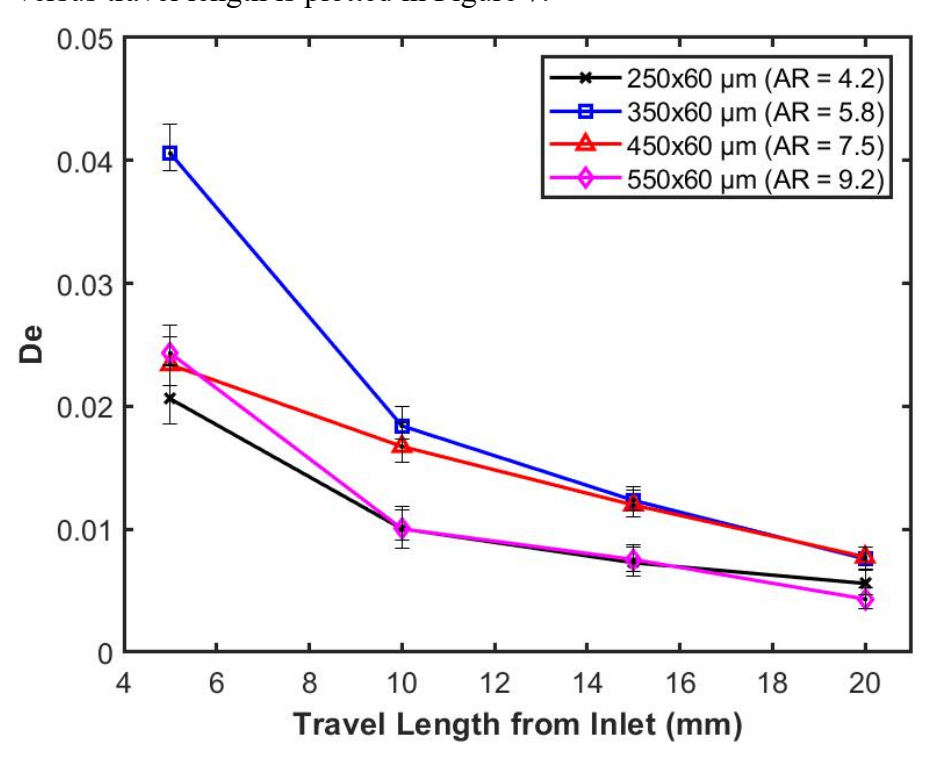


Figure 7. De at the different travel lengths from the spiral channel inlet in multiple microchannels with various sizes and aspect ratios.

This is the author's peer reviewed, accepted manuscript. However, the online version of record will be different from this version once it has been copyedited and typeset

The highest overall De was in the 5.8 aspect ratio spiral microchannel. Even though the De number is small compared to other Dean vortex-based separation devices with pump-controlled flow, the particles still experienced the Dean drag force applied by the secondary flow. Especially when the particles reached the lift-force equilibrium positions in the inertial migration, where the lift-force effects became negligible while the Dean drag force still exists and dominates the migration.

The 0.1% particle concentration BMF flows in the spiral microchannels with the inlet in the center and three outlets. Three spiral microchannels with different hydraulic diameter and aspect ratios were implemented in the experiments. The particles flowed into three independent branch outlets were recorded and counted. Figure 8 shows the particle distributions in the inner, middle, and outer branch outlets.

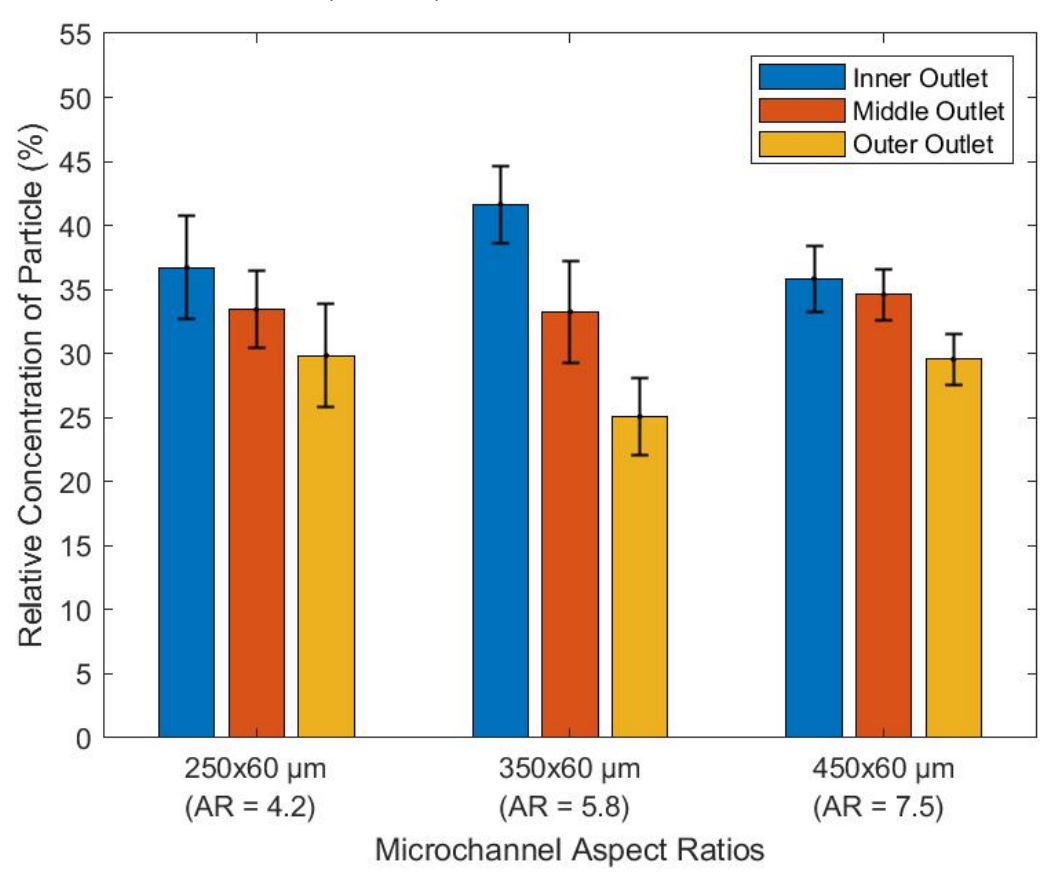


Figure 8. Particle distributions in the trifurcation branch outlets, more particles accumulated into the inner outlets.

This is the author's peer reviewed, accepted manuscript. However, the online version of record will be different from this version once it has been copyedited and typeset

The results of the blood mimicking fluid flow with particles prove that the particles also can be affected by the inertial focusing and Dean vortices in the capillary conditions. In the most studies in the inertial migration and Dean vortex applications in the microfluidic field, a high aspect ratio (W/H) microchannel with limited hydraulic diameter ( $a_p/D_h > 0.07$ , where  $a_p$  is diameter of particle for separation,  $D_h$  is hydraulic diameter of microchannel) [55]. However, in the capillary flow condition, the flow rate is sharply decreases with travel length in the microchannel [23], a microchannel that is capable to hold a higher Re meanwhile also has a relative higher aspect ratio is preferred for the Dean vortex implemented inertial microfluidic application.

From the results, the 5.8 aspect ratio spiral microchannel has the best performance for implementing the inertial focusing and Dean vortices in the microchannel to focus the particles to the inner side of microchannel. The high Re number make the particles inside the 5.8 aspect ratio spiral microchannel migrate to the equilibrium positions faster and enhance the Dean drag force to the particles. In the capillary flow, the flow rate keeps decreasing due to pressure drop caused by the increasing viscous force in the microchannel. The Re can not satisfy the inertial focusing requirement after ~25 mm travel length in the microchannels (~100 µm hydraulic diameter). Owing to this limitation, the particles can not fully migrated to the one side of the microchannel as they are in the flow with consistent high flow rates. The completion of the separation needs more travel length compared to the inertial focusing effective capillary flow. However, partial separation of the particles/blood cells still has the value in the microfluidic applications, especially the separation of the blood cells. The viscosity of the blood is highly dependent on its hematocrit (hct) and shear rate in the channel flow. The higher viscosity of the blood poses the challenge for the blood plasma filtration, typically in the capillary flow [37].

Porcine blood was used in the experiments for blood plasma separation. Distinct to the BMF, the blood is a shear thinning non-Newtonian fluid. That means the viscosity of blood flow will become higher in the low shear rate condition due to the RBC aggregation and deformation, while the viscosity will become lower until consistent in

PLEASE CITE THIS ARTICLE AS DOI: 10.1063/5.0189413

the high shear rate condition. Therefore, the viscosity of the blood flow is inconsistent owing to the changing of the shear rate in the capillary flow. On the other hand, the lateral forces acting on the RBCs will change due to the deformation of RBC during the flow, leading to variations in the focusing positions. These effects complicate the separation of blood plasma compared to separation in the BMF. As it is known that the hematocrit of blood samples significantly influences blood flow behavior, blood samples with varying hematocrit levels were utilized for blood plasma separation. The hematocrit quantification method in the microfluidic channel flow was developed and discussed in the previous study [56]. The blood samples with 30%, 35%, 40%, and 45% het were prepared for the experiments. 2 µl blood drops were introduced into the microchannel inlets, and the images of the branch outlet channels were recorded by the high-speed camera at the restricted condition. The hematocrit of the blood flow in the branch outlet channels was quantified using the grayscale information of the images of blood flow, as shown in Figure S1. And the hematocrit of the blood flows in the branch outlets are plotted in the figure 9.

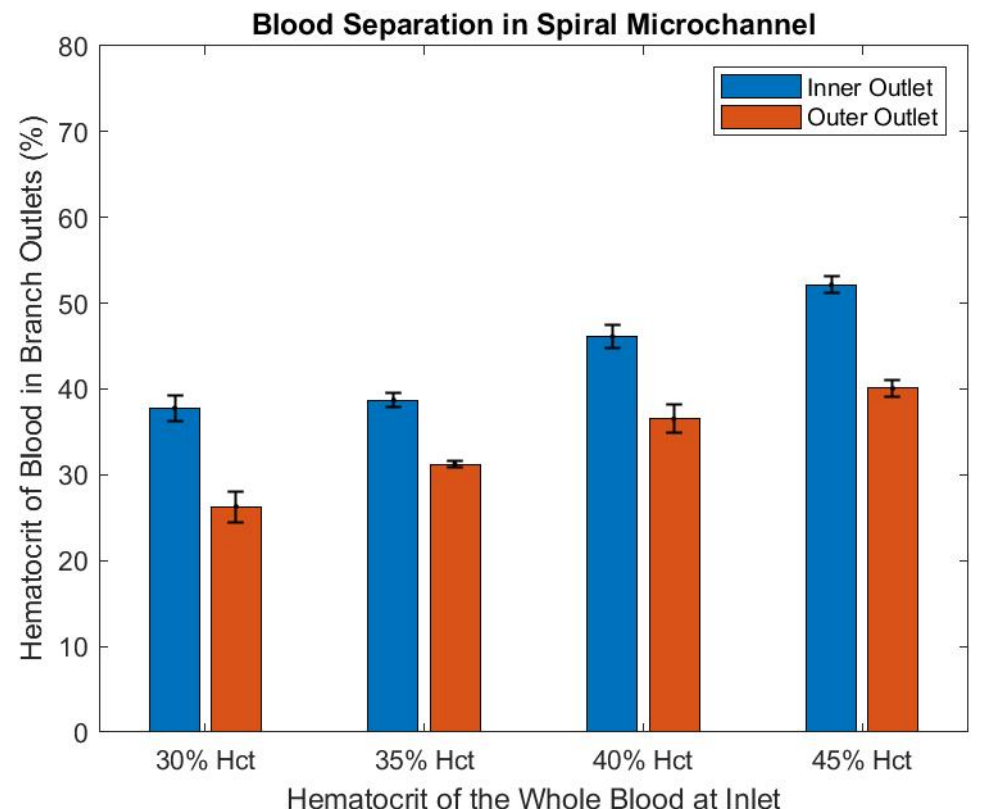


Figure 9. The blood cell focusing results of the 30%, 35%, 40%, and 45% hct blood

This is the author's peer reviewed, accepted manuscript. However, the online version of record will be different from this version once it has been copyedited and typeset

samples of the 5.8 aspect ratio spiral microchannel. The hematocrit variations in the branch outlets of the microchannel.

Within the physiological range of the blood samples, the inertial migration and Dean vortex effect of the blood cells in the capillary blood flow in the 5.8 aspect ratio spiral microchannel are still functional as they are in the BMF flow but less effective. More than 5% het decrease obtained with the 45% het samples. By incorporating a spiral microchannel and leveraging enhanced blood plasma separation through inertial migration and Dean vortex effects, the microfilter-based self-powered microfluidic device demonstrates faster and more efficient blood plasma separation. This results in a relatively higher volume of separated plasma and faster separation speeds, addressing issues such as clogging and pressure drops in microfilters, making this method suitable for Point-of-Care (POC) diagnosis applications compared to other existing technologies (Table 1). Consequently, the development of additional microfluidic-based POC diagnosis devices becomes viable, and the limit-of-detection issue is mitigated due to the increased separated plasma volume.

Table 1. Blood plasma separation characteristics by methods

Method	Volume range for separation	Separation time	Standalone capability
Conventional Centrifugation [57,58]	5-50 ml	10-30 mins	No, Bulky centrifuges needed
Microfluidic centrifugation [59,60]	100-2000 μ1	5-10mins	No, Motor & other power systems needed.
Microfiltration [13,14,28,30]	5-1000 μl	5-15 mins	Partial, some of them need external pumping system
Our Approach	2-5 μ1	< 1 min	Yes, no external device needed

#### **♦** Conclusions

In summary, this study investigated the focusing of porcine RBCs and RBC-sized particles through inertial migration and the Dean vortex effect within spiral microchannels, as well as the inertial migration of RBC-sized particles within straight

This is the author's peer reviewed, accepted manuscript. However, the online version of record will be different from this version once it has been copyedited and typeset

microchannels under capillary flow conditions. The experiments in straight microchannels showed that 88% of particles reached equilibrium positions, indicating the effectiveness of inertial migration in low-viscosity capillary flow. Notably, within the 5.8 aspect ratio spiral microchannel, a 23% relative concentration difference was observed between the inner and outer outlets, highlighting the significant particle migration during BMF capillary flow.

The particles have the rigid property and the actual size is bigger than the procine RBC, and the BMF has a relative lower and consistent viscosity compared to the blood flow. Due to these reasons, the particle migration during the BMF capillary flow is more notable.

In the context of blood flow experiments, the RBCs exhibited high deformability, impacting their behavior as opposed to behaving as rigid entities. The plasma environment led to RBC aggregation under low shear rate conditions, resulting in variable fluid viscosity and rendering the separation process less predictable. Consequently, many unexplored factors exist, and require further investigation to attain a more comprehensive understanding and improved modeling of RBC behavior during the capillary flow in the microfluidic channels under the combined influences of inertial focusing and secondary flow.

The differences in hematocrit levels between the inner and outer outlets in blood flow experiments are not as notable as in particle focusing experiments. However, a 5% -10% reduction in hematocrit yields a notable enhancement in the speed of blood plasma separation within the microfilters.

# **♦** Supplementary Material

See the supplementary material for the method to quantify the hematocrit value of the blood flow in the branch outlet.

PLEASE CITE THIS ARTICLE AS DOI: 10.1063/5.0189413

# ◆ Acknowledgments The authors acknowledge

The authors acknowledge the research support from the New Jersey Institute of Technology (NJIT) and the National Science Foundation (Grant ID: NSF 2318433). This research used the 3-D Laser Lithography System (Photonic Professional GT) of the Center for Functional Nanomaterials (CFN), which is a U.S. Department of Energy Office of Science User Facility, at Brookhaven National Laboratory under Contract No. DE-SC0012704.

#### **◆** Conflict of Interest Statement

The authors declare no conflict of interest.

# **◆** Author Contributions

Y. W. contributed to writing, conducting experiments, and editing the manuscript. N.T. contributed to assisting in experiments, and editing. B.B.N. contributed to review, and editing of the manuscript, and E.S.L. provided supervision, review, and guidance for this research paper. All authors have read and agreed to the published version of the manuscript.

# **♦** Data Availability

The data that support the findings of this study are available within the article and its supplementary material.

#### **◆** REFERENCES

- [1] Kim, H., Park, H., Chung, D.R., Kim, T., Park, E. and Kang, M., 2022. A self-pressure-driven blood plasma-separation device for point-of-care diagnostics. Talanta, 247, p.123562.
- [2] Herington, E. and MacDougall, D., 2021. Point-of-Care Testing of International Normalized Ratios for People on Oral Anticoagulants: A Rapid Qualitative Review. Canadian Journal of Health Technologies, 1(3).

- [3] Sachdeva, S., Davis, R.W. and Saha, A.K., 2021. Microfluidic point-of-care testing: commercial landscape and future directions. Frontiers in Bioengineering and Biotechnology, 8, p.602659.
  [4] Vashist, S.K., 2017. Point-of-care diagnostics: Recent advances and trends. Biosensors, 7(4), p.62.
  [5] Nunna, B.B., Mandal, D., Lee, J.U., Singh, H., Zhuang, S., Misra, D., Bhuyian,
  - [5] Nunna, B.B., Mandal, D., Lee, J.U., Singh, H., Zhuang, S., Misra, D., Bhuyian, M.N.U. and Lee, E.S., 2019. Detection of cancer antigens (CA-125) using gold nano particles on interdigitated electrode-based microfluidic biosensor. Nano convergence, 6, pp.1-12.
  - [6] Okorodudu, A.O., 2012. Optimizing accuracy and precision for point-of-care tests. Point of Care, 11(1), pp.26-29.
  - [7] Yang, S.M., Lv, S., Zhang, W. and Cui, Y., 2022. Microfluidic point-of-care (POC) devices in early diagnosis: A review of opportunities and challenges. Sensors, 22(4), p.1620.
  - [8] Seo, H.K., Kim, Y.H., Kim, H.O. and Kim, Y.J., 2010. Hybrid cell sorters for on-chip cell separation by hydrodynamics and magnetophoresis. *Journal of Micromechanics and Microengineering*, 20(9), p.095019.
  - [9] Mohammadi, M., Madadi, H., Casals-Terré, J. and Sellarès, J., 2015. Hydrodynamic and direct-current insulator-based dielectrophoresis (H-DC-iDEP) microfluidic blood plasma separation. *Analytical and bioanalytical chemistry*, 407, pp.4733-4744.
  - [10] JunáHuang, T., 2016. High-throughput acoustic separation of platelets from whole blood. *Lab on a Chip*, *16*(18), pp.3466-3472.
  - [11] Dow, P., Kotz, K., Gruszka, S., Holder, J. and Fiering, J., 2018. Acoustic separation in plastic microfluidics for rapid detection of bacteria in blood using engineered bacteriophage. *Lab on a Chip*, *18*(6), pp.923-932.
  - [12] Kolliopoulos, P. and Kumar, S., 2021. Capillary flow of liquids in open microchannels: overview and recent advances. npj Microgravity, 7(1), p.51.
  - [13] Dimov, I.K., Basabe-Desmonts, L., Garcia-Cordero, J.L., Ross, B.M., Ricco, A.J. and Lee, L.P., 2011. Stand-alone self-powered integrated microfluidic blood analysis system (SIMBAS). *Lab on a Chip*, *11*(5), pp.845-850.

- [14] Yeh, E.C., Fu, C.C., Hu, L., Thakur, R., Feng, J. and Lee, L.P., 2017. Self-powered integrated microfluidic point-of-care low-cost enabling (SIMPLE) chip. Science advances, 3(3), p.e1501645.
- [15] Olanrewaju, A., Beaugrand, M., Yafia, M. and Juncker, D., 2018. Capillary microfluidics in microchannels: from microfluidic networks to capillaric circuits. Lab on a Chip, 18(16), pp.2323-2347.
- [16] Nunna, B.B., Wang, Y., Talukder, N. and Lee, E.S., 2022, March. Capillary flow dynamics of blood with varied hematocrit in microfluidic platforms. In 2022 IEEE Healthcare Innovations and Point of Care Technologies (HI-POCT) (pp. 1-4). IEEE.
- [17] Maria, M.S., Rakesh, P.E., Chandra, T.S. and Sen, A., 2017. Capillary flow-driven microfluidic device with wettability gradient and sedimentation effects for blood plasma separation. Scientific reports, 7(1), p.43457.
- [18] Lee, M.G., Shin, J.H., Choi, S. and Park, J.K., 2014. Enhanced blood plasma separation by modulation of inertial lift force. Sensors and Actuators B: Chemical, 190, pp.311-317.
- [19] Rafeie, M., Zhang, J., Asadnia, M., Li, W. and Warkiani, M.E., 2016. Multiplexing slanted spiral microchannels for ultra-fast blood plasma separation. Lab on a *Chip*, 16(15), pp.2791-2802.
- [20] Robinson, M., Marks, H., Hinsdale, T., Maitland, K. and Coté, G., 2017. Rapid isolation of blood plasma using cascaded inertial microfluidic device. Biomicrofluidics, 11(2).
- [21] Ardhapurkar, P.M., Sridharan, A. and Atrey, M.D., 2014, January. Investigation of pressure drop in capillary tube for mixed refrigerant Joule-Thomson cryocooler. In AIP Conference Proceedings (Vol. 1573, No. 1, pp. 155-162). American Institute of Physics.
- [22] Cai, J., Jin, T., Kou, J., Zou, S., Xiao, J. and Meng, Q., 2021. Lucas-Washburn equation-based modeling of capillary-driven flow in porous systems. Langmuir, 37(5), pp.1623-1636.
- [23] Washburn, E.W., 1921. The dynamics of capillary flow. Physical review, 17(3), p.273.
- [24] Rivero-Rodriguez, J. and Scheid, B., 2018. Bubble dynamics in microchannels: inertial and capillary migration forces. Journal of fluid mechanics, 842, pp.215-247.

PLEASE CITE THIS ARTICLE AS DOI: 10.1063/5.0189413

- [25] Wang, Y., Nunna, B.B., Talukder, N., Etienne, E.E. and Lee, E.S., 2021. Blood plasma self-separation technologies during the self-driven flow in microfluidic platforms. Bioengineering, 8(7), p.94.
- [26] Nam, Y., Kim, M. and Kim, T., 2014. Pneumatically controlled multi-level microchannel for separation and extraction of microparticles. Sensors and Actuators B: Chemical, 190, pp.86-92.
- [27] Didar, T.F., Li, K., Tabrizian, M. and Veres, T., 2013. High throughput multilayer microfluidic particle separation platform using embedded thermoplastic-based micropumping. Lab on a Chip, 13(13), pp.2615-2622.
- [28] Karimi, S., Mojaddam, M., Majidi, S., Mehrdel, P., Farré-Lladós, J. and Casals-Terré, J., 2021. Numerical and experimental analysis of a high-throughput blood plasma separator for point-of-care applications. Analytical and bioanalytical chemistry, 413, pp.2867-2878.
- [29] Yoon, Y., Lee, J., Ra, M., Gwon, H., Lee, S., Kim, M.Y., Yoo, K.C., Sul, O., Kim, C.G., Kim, W.Y. and Park, J.G., 2019. Continuous separation of circulating tumor cells from whole blood using a slanted weir microfluidic device. Cancers, 11(2), p.200.
- [30] Hauser, J., Lenk, G., Hansson, J., Beck, O., Stemme, G. and Roxhed, N., 2018. High-yield passive plasma filtration from human finger prick blood. Analytical chemistry, 90(22), pp.13393-13399.
- [31] Spigarelli, L., Bertana, V., Marchisio, D., Scaltrito, L., Ferrero, S., Cocuzza, M., Marasso, S.L., Canavese, G. and Pirri, C.F., 2019. A passive two-way microfluidic device for low volume blood-plasma separation. Microelectronic Engineering, 209, pp.28-34.
- [32] Al-Aqbi, Z.T., Albukhaty, S., Zarzoor, A.M., Sulaiman, G.M., Khalil, K.A., Belali, T. and Soliman, M.T., 2021. A novel microfluidic device for blood plasma filtration. Micromachines, 12(3), p.336.
- [33] Enten, A.C., Leipner, M.P., Bellavia, M.C., King, L.E. and Sulchek, T.A., 2020. Optimizing flux capacity of dead-end filtration membranes by controlling flow with pulse width modulated periodic backflush. Scientific Reports, 10(1), p.896.
- [34] Chiu, Y.Y., Huang, C.K. and Lu, Y.W., 2016. Enhancement of microfluidic particle separation using cross-flow filters with hydrodynamic focusing. Biomicrofluidics, 10(1).

- [35] Eckmann, D.M., Bowers, S., Stecker, M. and Cheung, A.T., 2000. Hematocrit, volume expander, temperature, and shear rate effects on blood viscosity. Anesthesia & Analgesia, 91(3), pp.539-545.
- [36] Picart, C., Piau, J.M., Galliard, H. and Carpentier, P., 1998. Human blood shear yield stress and its hematocrit dependence. Journal of Rheology, 42(1), pp.1-12.
- [37] Weiss, D.J., Evanson, O. and Geor, R.J., 1994. Filterability of equine erythrocytes and whole blood: Effects of haematocrit, pore size and flow rate. Comparative haematology international, 4, pp.11-16.
- [38] Piety, N.Z., Reinhart, W.H., Stutz, J. and Shevkoplyas, S.S., 2017. Optimal hematocrit in an artificial microvascular network. Transfusion, 57(9), pp.2257-2266.
- [39] Reinhart, W.H., Piety, N.Z. and Shevkoplyas, S.S., 2017. Influence of feeding hematocrit and perfusion pressure on hematocrit reduction (Fåhraeus effect) in an artificial microvascular network. Microcirculation, 24(8), p.e12396.
- [40] Aran, K., Fok, A., Sasso, L.A., Kamdar, N., Guan, Y., Sun, Q., Ündar, A. and Zahn, J.D., 2011. Microfiltration platform for continuous blood plasma protein extraction from whole blood during cardiac surgery. Lab on a Chip, 11(17), pp.2858-2868.
- [41] Hossain, M.M.N., Hu, N.W., Abdelhamid, M., Singh, S., Murfee, W.L. and Balogh, P., 2023. Angiogenic Microvascular Wall Shear Stress Patterns Revealed Through Three-dimensional Red Blood Cell Resolved Modeling. Function, 4(6), p.zqad046.
- [42] Nader, E., Skinner, S., Romana, M., Fort, R., Lemonne, N., Guillot, N., Gauthier, A., Antoine-Jonville, S., Renoux, C., Hardy-Dessources, M.D. and Stauffer, E., 2019. Blood rheology: key parameters, impact on blood flow, role in sickle cell disease and effects of exercise. Frontiers in physiology, 10, p.1329.
- [43] Ullah, A., Holdich, R.G., Naeem, M. and Starov, V.M., 2012. Shear enhanced microfiltration and rejection of crude oil drops through a slotted pore membrane including migration velocities. Journal of Membrane science, 421, pp.69-74.
- [44] Loong, E.D., 1980. Microfiltration of stored blood. Anaesthesia and Intensive Care, 8(2), pp.158-161.
- [45] Di Carlo, D., Edd, J.F., Irimia, D., Tompkins, R.G. and Toner, M., 2008. Equilibrium separation and filtration of particles using differential inertial focusing. Analytical chemistry, 80(6), pp.2204-2211.

- [46] Di Carlo, D., Irimia, D., Tompkins, R.G. and Toner, M., 2007. Continuous inertial focusing, ordering, and separation of particles in microchannels. Proceedings of the National Academy of Sciences, 104(48), pp.18892-18897.
- [47] Lee, L.M., Bhatt, K.H., Haithcock, D.W. and Prabhakarpandian, B., 2023. Blood component separation in straight microfluidic channels. Biomicrofluidics, 17(5).
- [48] Zhou, J. and Papautsky, I., 2013. Fundamentals of inertial focusing in microchannels. Lab on a Chip, 13(6), pp.1121-1132.
- [49] Zhang, J., Yan, S., Yuan, D., Alici, G., Nguyen, N.T., Warkiani, M.E. and Li, W., 2016. Fundamentals and applications of inertial microfluidics: A review. Lab on a Chip, 16(1), pp.10-34.
- [50] Abbas, M., Magaud, P., Gao, Y. and Geoffroy, S., 2014. Migration of finite sized particles in a laminar square channel flow from low to high Reynolds numbers. Physics of Fluids, 26(12).
- [51] Zhou, J., Peng, Z. and Papautsky, I., 2020. Mapping inertial migration in the cross section of a microfluidic channel with high-speed imaging. Microsystems & Nanoengineering, 6(1), p.105.
- [52] Cappello, J., Rivero-Rodríguez, J., Vitry, Y., Dewandre, A., Sobac, B. and Scheid, B., 2023. Beads, bubbles and drops in microchannels: stability of centred position and equilibrium velocity. Journal of Fluid Mechanics, 956, p.A21.
- [53] Bhagat, A.A.S., Kuntaegowdanahalli, S.S. and Papautsky, I., 2008. Enhanced particle filtration in straight microchannels using shear-modulated migration. Physics of Fluids, 20(10).
- [54] Dean, W.R., 1927. XVI. Note on the motion of fluid in a curved pipe. The London, Edinburgh, and Dublin Philosophical Magazine and Journal of Science, 4(20), pp.208-223.
- [55] Guan, G., Wu, L., Bhagat, A.A., Li, Z., Chen, P.C., Chao, S., Ong, C.J. and Han, J., 2013. Spiral microchannel with rectangular and trapezoidal cross-sections for size based particle separation. Scientific reports, 3(1), p.1475.
- [56] Wang, Y., Nunna, B.B., Talukder, N. and Lee, E.S., 2022. Microfluidic-Based Novel Optical Quantification of Red Blood Cell Concentration in Blood Flow. Bioengineering, 9(6), p.247.

This is the author's peer reviewed, accepted manuscript. However, the online version of record will be different from this version once it has been copyedited and typeset.

- [57] Rinsler, M.G., 1981. Clinical diagnosis and management by laboratory methods. Journal of Clinical Pathology, 34(2), p.228.
- [58] Thavasu, P.W., Longhurst, S., Joel, S.P., Slevin, M.L. and Balkwill, F.R., 1992. Measuring cytokine levels in blood. Importance of anticoagulants, processing, and storage conditions. Journal of immunological methods, 153(1-2), pp.115-124.
- [59] Wong, A.P., Gupta, M., Shevkoplyas, S.S. and Whitesides, G.M., 2008. Egg beater as centrifuge: isolating human blood plasma from whole blood in resource-poor settings. Lab on a Chip, 8(12), pp.2032-2037.
- [60] Amasia, M. and Madou, M., 2010. Large-volume centrifugal microfluidic device for blood plasma separation. Bioanalysis, 2(10), pp.1701-1710.